Icarus 408 (2024) 115826

Contents lists available at ScienceDirect

Icarus

journal homepage: www.elsevier.com/locate/icarus

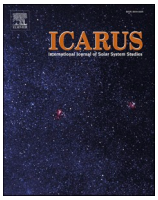

The thermal history of Ryugu based on Raman characterization of Hayabusa2 samples

Lydie Bonal [a,*], Eric Quirico [a], Gilles Montagnac [b], Mutsumi Komatsu [c,d], Yoko Kebukawa [e], Hikaru Yabuta [f], Kana Amano [g], Jens Barosch [h], Laure Bejach [i], George D. Cody [h], Emmanuel Dartois [j], Alexandre Dazzi [k], Bradley De Gregorio [l], Ariane Deniset-Besseau [k], Jean Duprat [m], Cécile Engrand [i], Minako Hashiguchi [n], Kanami Kamide [f], David Kilcoyne [o,1], Zita Martins [p], Jérémie Mathurin [k], Smail Mostefaoui [m], Larry Nittler [h], Takuji Ohigashi [q], Taiga Okumura [r], Laurent Remusat [m], Scott Sandford [s], Miho Shigenaka [f], Rhonda Stroud [l], Hiroki Suga [t], Yoshio Takahashi [r,u], Yasuo Takeichi [u], Yusuke Tamenori [t], Maximilien Verdier-Paoletti [m], Shohei Yamashita [u], Tomoki Nakamura [g], Hiroshi Naraoka [v], Takaaki Noguchi [w], Ryuji Okazaki [v], Hisayoshi Yurimoto [x], Shogo Tachibana [y], Masanao Abe [z], Akiko Miyazaki [z], Aiko Nakato [z], Satoru Nakazawa [z], Masahiro Nishimura [z], Tatsuaki Okada [z], Takanao Saiki [z], Kanako Sakamoto [z], Satoshi Tanaka [z], Fuyuto Terui [aa], Yuichi Tsuda [z], Tomohiro Usui [z], Sei-ichiro Watanabe [ab], Toru Yada [z], Kasumi Yogata [z], Makota Yoshikawa [z]

[a] *Institut de Planétologie et d'Astrophysique, Université Grenoble Alpes, 38000 Grenoble, France*
[b] *École normale supérieure de Lyon, University Lyon 1, Lyon Cedex 07 69342, France*
[c] *Center for University-Wide Education, Saitama Prefectural University, Saitama 343-8540, Japan*
[d] *Department of Earth Sciences, Waseda University, Shinjuku-ku, Tokyo 169-8050, Japan*
[e] *Faculty of Engineering, Yokohama National University, Yokohama 240-8501, Kanagawa, Japan*
[f] *Department of Earth and Planetary Systems Science, Hiroshima University, Higashi-Hiroshima, Hiroshima 739-8526, Japan*
[g] *Tohoku University, Sendai 980-8578, Japan*
[h] *Earth and Planets Laboratory, Carnegie Institution for Science, Washington, DC 20015, USA*
[i] *IJCLab, UMR 9012 Université Paris-Saclay/CNRS, 91405 Orsay, France*
[j] *Institut des Sciences Moléculaires d'Orsay (ISMO), UMR8214, Université Paris-Saclay/CNRS, 91405 Orsay, France*
[k] *Institut Chimie Physique (ICP), UMR 8000, Université Paris-Saclay/CNRS, 91405 Orsay, France*
[l] *Materials Science and Technology Division, US Naval Research Laboratory, Washington, DC 20375, USA*
[m] *Institut de Minéralogie, Physique des Matériaux et Cosmochimie, Museum National d'Histoire Naturelle, UMR CNRS 7590, Sorbonne Université, Paris Cedex 05 75231, France*
[n] *Graduate School of Environmental Studies, Nagoya University, Chikusa-ku, Nagoya 464-8601, Japan*
[o] *Advanced Light Source, Lawrence Berkeley National Laboratory, Berkeley, CA 94720-8229, USA*
[p] *Centro de Química Estrutural, Institute of Molecular Sciences and Department of Chemical Engineering, Instituto Superior Técnico, Universidade de Lisboa, Av. Rovisco Pais 1, 1049-001 Lisboa, Portugal*
[q] *Institute for Molecular Science, UVSOR Synchrotron Facility, Myodaiji, Okazaki 444-8585, Japan*
[r] *Department of Earth and Planetary Science, The University of Tokyo, Bunkyo-ku, Tokyo 113-0033, Japan*
[s] *NASA Ames Research Center, Moffett Field, CA 94035-1000, USA*
[t] *Japan Synchrotron Radiation Research Institute (JASRI), Sayo-gun, Hyogo 679-5198, Japan*
[u] *Institute of Materials Structure Science, High Energy Accelerator Research Organization, KEK, Tsukuba, Ibaraki, 305-0801, Japan*
[v] *Kyushu University, Fukuoka 812-8581, Japan*
[w] *Kyoto University, Kyoto 606-8502, Japan*
[x] *Hokkaido University, Sapporo 060-0810, Japan*
[y] *The University of Tokyo, Tokyo 113-0033, Japan*
[z] *Institute of Space and Astronautical Science (ISAS), Japan Aerospace Exploration Agency (JAXA), Sagamihara 252-5210, Japan*
[aa] *Kanagawa Institute of Technology, Atsugi 243-0292, Japan*
[ab] *Nagoya University, Nagoya 464-8601, Japan*

* Corresponding author.
E-mail address: lydie.bonal@univ-grenoble-alpes.fr (L. Bonal).
[1] Deceased.

https://doi.org/10.1016/j.icarus.2023.115826
Received 15 November 2022; Received in revised form 29 September 2023; Accepted 2 October 2023
Available online 5 October 2023

ARTICLE INFO

Keywords:
Asteroid Ryugu
Thermal histories
Geological processes
Spectroscopy
Meteorites

ABSTRACT

This paper is focused on the characterization of the thermal history of C-type asteroid Ryugu through the structure of the polyaromatic carbonaceous matter in the returned samples determined by Raman spectroscopy. Both intact particles and extracted Insoluble Organic Matter (IOM) from the two sampling sites on Ryugu have been characterized. The main conclusions are that *(i)* there is no structural difference of the polyaromatic component probed by Raman spectroscopy between the two sampling sites, *(ii)* in a manner similar to type 1 and 2 chondrites, the characterized Ryugu particles did not experience significant long-duration thermal metamorphism related to the radioactive decay of elements such as ^{26}Al; *(iii)* some structural variability is nevertheless observed within our particle set. It can be interpreted as some particles having experienced some short-duration and weak heating (R3 in the scale defined by Quirico et al. 2018 and TII or lower according to the scale defined by Nakamura, 2005).

1. Introduction

C-complex asteroids are the dominating population in the asteroid belt, representing ~60% of its mass (DeMeo and Carry, 2014, 2013). They are typically linked to primitive, volatile-rich carbonaceous chondrites (e.g., DeMeo et al., 2015). These small bodies and all the derived cosmomaterials (meteorites, potentially some dust as Interplanetary Dust Particles and micro-meteorites) are thus key-objects to investigate the formation and evolution of the Solar System. Nevertheless, as primitive as they are, all of these small bodies have experienced some processing since their formation. These processes may have modified their surface (space weathering), but also the composition of the whole body through geological post-accretion processes (thermal and shock metamorphism, and aqueous alteration). It is thus indispensable to identify each of the experienced processes to understand the induced modifications and avoiding the risk of mis- or over-interpreting some properties of primitive bodies and cosmomaterials.

Ryugu, a C-type asteroid, has been visited by the JAXA's Hayabusa2 spacecraft. During more than a year, remote (e.g., Watanabe et al., 2019) and in situ (e.g., Ho et al., 2021) characterizations were undertaken, two touchdowns at different sites (e.g., Tsuda et al., 2020) and an impact experiment (Arakawa et al., 2020) were performed. In December 2020, after the sample recovery capsule was cautiously opened, 5.42 g of samples collected at the surface of Ryugu were discovered (Yada et al., 2022). Starting in June 2021 and for a period of one year, several teams (so called "Phase2 curation teams" and "Hayabusa2 Initial Analysis Team" (IAT)) had the opportunity to work on these samples. In particular, the Hayabusa2 IAT consisting of six specialized sub-teams were dedicated to achieve the scientific objectives of Hayabusa2 through the high-precision analyses of the asteroid samples. In particular, the Initial Analysis Organic Macromolecule team (PI: H. Yabuta) performed comprehensive analysis to unveil the elemental, isotopic, and functional group compositions, structures and morphologies of macromolecular organic matter from the Ryugu samples (Yabuta et al., 2023). The degree of structural order of the polyaromatic carbonaceous matter present in extraterrestrial samples is a tracer of the thermal history they experienced (e.g., primitive chondrites: e.g., Bonal et al., 2016, 2006; Busemann et al., 2007; Quirico et al., 2018; micrometeorites: Battandier et al., 2018; Dobrică et al., 2011). To characterize Ryugu thermal history (long vs. short thermal heating and its extent), we thus performed Raman characterization of several samples returned by the Hayabusa2 mission and compared the spectral parameters with those of reference chondrites.

Table 1
Hayabusa2-samples list.

	sample name	raw	IOM
Chamber A	aggregate A0106-4		
	aggregate A0106-6		
	aggregate A0106-23, 24, 25 (✣)		*
	A0106_IOM residue		
	aggregate A0108-6		
	aggregate A0108-10		*
	aggregate A0108-18		
	aggregate A0108-61		
Chamber C	aggregate C0109-5		*
	aggregate C0109-9		
	aggregate C0109-12		*
	individual particle C0057-6		*
	individual particle C0002		*
	C0107_IOM residue		

IOM stands for Insoluble Organic Matter, either chemically extracted by H. Yabuta (PI of PET IOM) or in IPAG (*, see Section 2.1 for explanations). (✣) the three individual particles moved during their trip between Japan and France. The identification of the exact particle that we characterized was thus not possible.

2. Samples and methods

2.1. Samples

In the curation facility, *individual particles* (typical size of the particles is 1–2 mm) were picked out from the whole Hayabusa2 sample set and the remaining sample mass was separated in several sets of *aggregate samples* (~10 mg each) made of numerous small particles (see for example, guidebook for proposers on the website of Announcement of Opportunity for Ryugu samples and Ryugu Sample Database System). In the present work, whole particles from Chamber A aggregates collected upon the first touchdown and Chamber C aggregates collected upon the second touchdown and also fragments of *individual particles* from Chamber C were characterized. The sample numbers are all listed in Table 1. In addition to samples dedicated to the Organic Macromolecule team, we had the opportunity to work on the individual particle C0002 from Stone team (PI. T. Nakamura), which was from Chamber C and the third largest grain among all the returned sample.

In addition to intact samples, Insoluble Organic Matter (IOM) chemically extracted from several aggregates and individual particles were also characterized. Indeed, IOM was extracted from *(i)* individual fragments of Ryugu particles in IPAG (Grenoble, France) (see Quirico et al., 2022 and corresponding paper Quirico et al., accepted for details on the chemical protocol) and, *(ii)* from the bulk aggregates A0106 and C0107 in Hiroshima University by H. Yabuta (sample names described with the extension (HY) in the text).

In addition to Ryugu samples, a series of primitive chondrites (Table 2) were characterized and analyzed in the exact same experimental and analytical conditions as for Ryugu samples. Although these chondrites had been analyzed in previous work (e.g. Quirico et al., 2018), they were again characterized here to ease and fully legitimate a

Table 2
Primitive chondrites measured for spectral comparison.

	Chondrite	Classification
Types 1 and 2 chondrites	ALH 84033	CM2
	AMH 84044	CM2
	Cold Bokkeveld	CM2
	EET 83355	C2-Ung
	EET 87522	CM2
	EET 96029	CM2
	LEW 87022	CM2
	MAC 88100	CM2
	MET 01070	CM1
	Murchison	CM2
	Nogoya	CM2
	Orgueil	CI1
	PCA 91008	CM2-an
	PCA 02012	CM2
	QUE 93005	CM2-an
	WIS 91600	CM-an
Type 3 chondrites	Bishunpur	LL3
	Chainpur	LL3
	EET 90628	L3
	Krymka	LL3
	QUE 97008	L3
	St Mary's County	LL3
	Hallingeberg	L3

ALH stands for Allan Hills, EET for Elephant Moraine, LEW for Lewis Cliff, MAC for MacAlpine Hills, MET for Meteorite Hills, PCA for Pecora Escarpment, QUE for Queen Alexandra Range and WIS for Wisconsin Range.

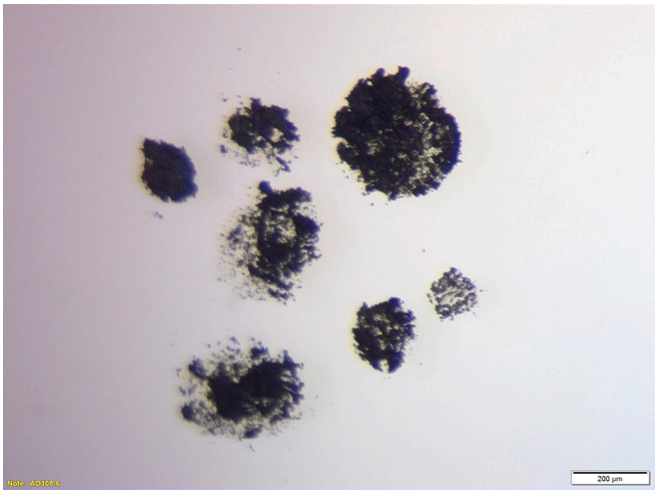

Fig. 1. Optical image of a preparation for Raman characterization of the Ryugu intact particle A0108-6. Several fragments were manually picked up and pressed between two glass slides.

subsequent comparison of their spectral parameters (see Section 3.1 for justification). Chondrites were prepared in a similar manner as Hayabusa2 samples. Matrix fragments (typical apparent diameter around 30 µm) were carefully selected manually according to colour and texture under a binocular microscope. The selected matrix grains were pressed between two glass slides that were also used as substrates for the Raman analysis, once separated.

2.2. Raman spectral acquisition

Over the time period dedicated to the characterization of some Ryugu samples within the Organic Macromolecule team, the Raman micro-spectrometer originally used (LabRAM HR800) and described in (Bonal et al., 2022) and Yabuta et al. (2023) has stopped working. It was then renewed in the middle of the time period dedicated to initial analysis. New measurements on the same Ryugu particles and additional ones were thus performed with another Raman spectrometer (LabRAM HR800 Evolution) for the present work. This is the reason why the average parameters reported here are slightly different from those in previous publications (Bonal et al. (2022) and Yabuta et al. (2023)). This difference is discussed in Section 3.1.

The Raman spectra were acquired with a 532 nm laser. Because some Raman bands related to carbonaceous matter are dispersive, data for Ryugu samples and meteorites (used as references for comparison of spectral parameters) have been acquired and analyzed along a given set of parameters. Raman measurements were performed at the Ecole Normale Supérieure de Lyon (Laboratoire de Géologie de Lyon—Terre, Planètes, Environnement) using a LabRAM HR800 Evolution Raman spectrometer (Horiba) equipped with a 600 g/mm grating centered at 1400 cm^{-1} giving access to the spectral region 500–2200 cm^{-1}. The laser was focused through a 100× objective to obtain a < 2 µm spot size. The power on the sample was 0.3 mW. Each acquisition comprised six integrations of 15 s that were averaged to make the final spectrum. One to three spectra were acquired per fragment and typically ten fragments of each particle of a given aggregate or individual particle were prepared (Fig. 1). The samples were either pressed on diamonds (for allowing subsequent infrared and/or NanoSIMS measurements) or on microscope glass slides.

2.3. Raman spectral analysis

The Raman spectra acquired on Ryugu samples considered in the present work systematically exhibit the so-called D- and G-bands related to the presence of polyaromatic carbonaceous matter. A linear baseline correction of the spectra between 1000 and 1700 cm^{-1} was systematically subtracted. The G- and D-bands were fitted with a Breit–Wigner–Fano and a Lorentzian profiles, respectively. The position (ω), maximum intensity, peak intensity (I) and full width at half maximum (FWHM) of the D- and G-bands were determined for each spectrum. For every sample, the mean value and 1 σ-standard deviation of each of these parameters were calculated.

3. Results

3.1. Particularities of Raman characterization of carbonaceous material

Raman spectroscopy is a technique that is relatively easy and fast to implement for characterization of a large set of samples. However, as it has been underlined in several papers, Raman spectroscopy on carbonaceous material presents several particularities that users have to be aware of. First, chondritic carbonaceous matter is opaque: it is characterized by a high extinction coefficient of the visible light. Therefore, the Raman scattering originates only from a thin surface layer of the sample: several tens to one hundred nm of the carbonaceous material (Lespade et al., 1984). This leads to a high sensitivity of the carbonaceous material to laser-induced heating. It is thus required to use low laser power on the surface of the sample to avoid artificially induced modification of the structural order of the carbonaceous matter, leading to a potential misinterpretation of its thermal history. Complicating this picture, even in the lack of thermal damages, the superficial region of the sample can be heated, leading to spectra with significant differences with those collected at room temperature and drift of the spectral parameters. Reproducibility of the instrument parameters and of the sample preparation procedure are then key to collect reliable Raman data.

Second, the D band is dispersive: its intensity and position vary with the energy of the incident photons. For visible excitation wavelengths, the position of the D band varies with the incident energy at a rate of 50 cm^{-1} eV^{-1} (Matthews et al., 1999; Pócsik et al., 1998). Although not dispersive in graphite, the G band is dispersive in disordered carbonaceous material, in which the dispersion is proportional to the degree of order (Ferrari and Robertson, 2000). The dispersion of the Raman bands relative to the excitation wavelengths of the incident laser prevents the

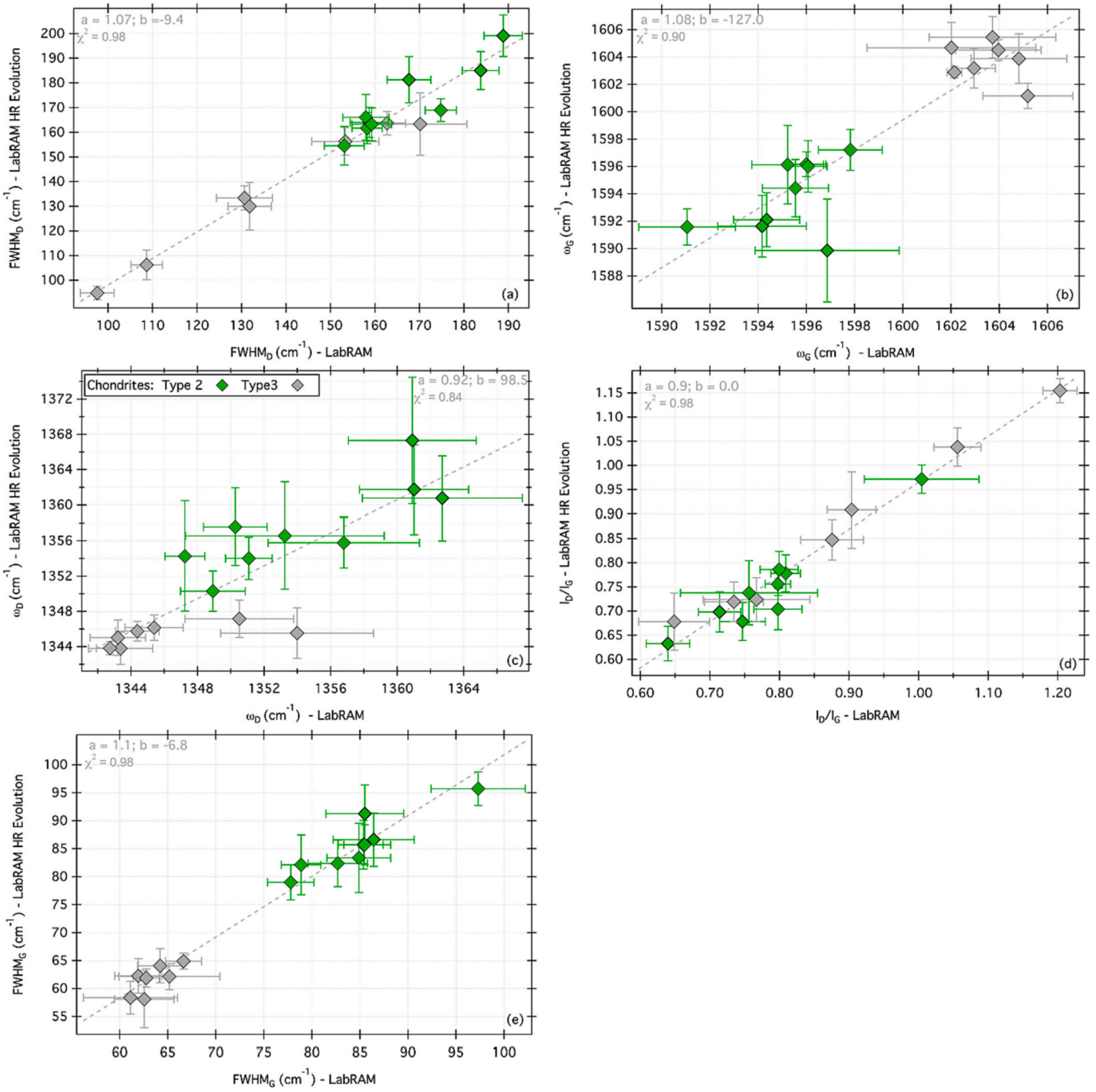

Fig. 2. Comparison of the numerical values of distinct average spectral parameters computed from Raman spectra acquired with two distinct instruments (so-called LabRAM and LabRAM HR Evolution) (see Section 2.2 for explanations) on a series of type 3 chondrites (in grey) and type 2 chondrites (in green). The dotted line figures the linear regression (y = ax + b). The absolute values of the spectral parameters obtained with the two instruments on the same samples are thus different but consistent. (For interpretation of the references to colour in this figure legend, the reader is referred to the web version of this article.)

definition of an absolute scale of Raman spectral parameters for chondrites. In other words, the numerical comparison of spectral parameters obtained for a sample with those obtained in other experimental conditions may be misleading, even if only G-band spectral parameters are considered. For a comparison to be meaningful, the Raman spectra have to be acquired in the same experimental conditions and the spectral parameters through a given analytical procedure. Nevertheless, various sets of spectral parameters obtained on similar samples with different Raman systems are consistent. Indeed, as mentioned earlier, two Raman spectrometers have been used in the timeframe of the present work: spectral parameters obtained on bulk matrix fragments of a series of chondrites with the so-called "LabRAM HR800" and "LabRAM HR800 Evolution" Raman micro-spectrometers are well correlated (Fig. 2, Table A1). The absolute values of the spectral parameters are different between Yabuta et al. (2023) and the present work but consistent: indeed, the interpretation in terms of relative metamorphic grade of this series of chondrites is independent from the considered Raman dataset.

3.2. Spectral analysis

In previous work, the baseline correction was led between 700 and 2000 cm^{-1} (e.g., Bonal et al., 2016) or 800 and 2000 cm^{-1} (e.g., Quirico

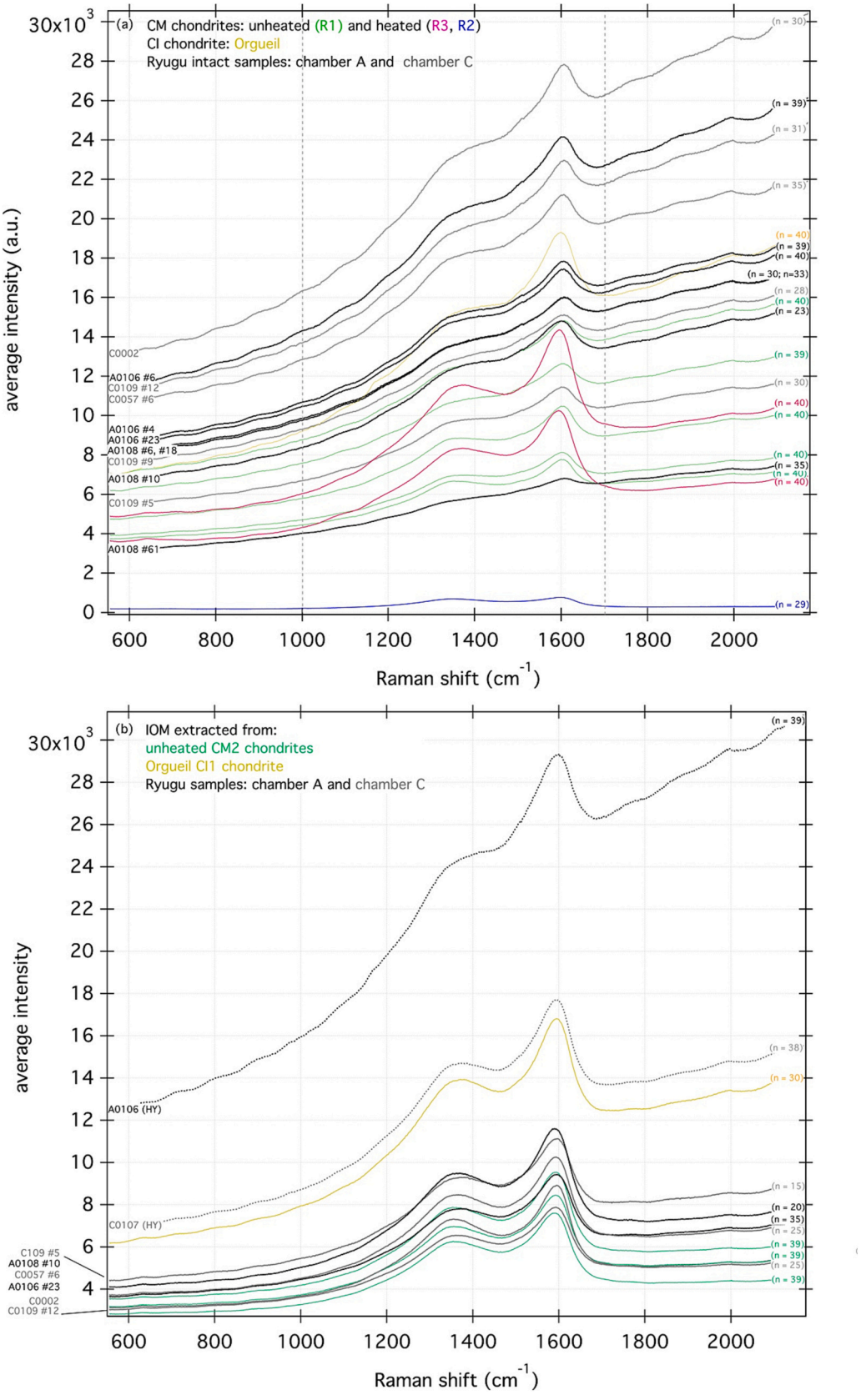

(caption on next page)

Fig. 3. Comparison of average Raman spectra of (a) individual intact Ryugu particles and of matrix fragments of types 1 and 2 chondrites (unheated in green and heated in magenta and blue) and (b) insoluble organic matter extracted from Ryugu samples and chondrites. Most of the IOMs were chemically extracted from individual fragments of intact Ryugu particles at IPAG (plain line), at the exception of two IOM (dotted lines) extracted by H. Yabuta. The number of individual spectra is indicated between parenthesis. "R1" (in green), "R3" (in magenta), and "R2" (in blue) designate unheated, moderately heated and heated type 2 chondrites, respectively (see Section 4.2. for explanation and Quirico et al., 2018). (For interpretation of the references to colour in this figure legend, the reader is referred to the web version of this article.)

Table 3
Hayabusa2 intact particles and extracted IOM considered in the present work and their respective spectral parameters.

	Sample name	sample type	n	$FWHM_D$ (cm^{-1})	I_D/I_G	$FWHM_G$ (cm^{-1})	ω_D (cm^{-1})	ω_G (cm^{-1})
Chamber A	aggregate A0106–4	intact part.	39	162.6 ± 5.8	0.74 ± 0.04	87.8 ± 5.2	1357.5 ± 4.3	1594.9 ± 1.3
	aggregate A0106–6	intact part.	30	162.0 ± 7.2	0.69 ± 0.05	91.9 ± 6.2	1359.7 ± 7.1	1592.4 ± 2.2
	aggregate A0106–23, 24, 25	intact part.	40	160.7 ± 5.5	0.75 ± 0.03	89.1 ± 5.2	1356.4 ± 5.9	1594.2 ± 1.5
		IOM	25	171.1 ± 4.5	0.69 ± 0.03	91.5 ± 3.0	1357.6 ± 2.3	1589.6 ± 2.0
	aggregate A0108–6	intact part.	30	161.5 ± 8.9	0.74 ± 0.04	90.2 ± 7.1	1358.9 ± 4.8	1594.4 ± 2.0
	aggregate A0108–10	intact part.	23	174.9 ± 9.8	0.70 ± 0.05	98.2 ± 5.1	1363.9 ± 7.2	1587.9 ± 3.2
		IOM	20	174.0 ± 3.0	0.69 ± 0.01	92.7 ± 2.2	1356.6 ± 1.9	1587.0 ± 0.9
	aggregate A0108–18	intact part.	33	164.3 ± 7.6	0.75 ± 0.02	89.9 ± 4.7	1359.7 ± 4.8	1595.0 ± 1.4
	aggregate A0108–61	intact part.	33	162.4 ± 8.1	0.70 ± 0.04	95.0 ± 8.2	1363.3 ± 8.3	1592.1 ± 2.7
	A0106_IOM residue	IOM*	41	162.6 ± 11.1	0.61 ± 0.06	96.3 ± 6.6	1353.5 ± 3.7	1586.8 ± 3.7
Chamber C	aggregate C0109–5	intact part.	30	162.7 ± 7.0	0.73 ± 0.02	89.6 ± 5.3	1355.8 ± 3.7	1593.0 ± 2.9
	aggregate C0109–9	intact part.	28	168.4 ± 6.88	0.68 ± 0.08	100.5 ± 8.1	1360.1 ± 4.0	1589.8 ± 3.9
	aggregate C0109–12	intact part.	25	159.6 ± 6.5	0.72 ± 0.04	83.3 ± 7.4	1359.0 ± 6.6	1595.7 ± 2.1
		IOM	25	173.7 ± 3.3	0.71 ± 0.01	92.9 ± 3.0	1359.4 ± 2.9	1589.1 ± 1.5
	individual particle C0057–6	intact part.	35	165.8 ± 8.7	0.77 ± 0.04	89.3 ± 7.4	1358.7 ± 8.2	1593.7 ± 2.1
		IOM	25	170.3 ± 2.4	0.71 ± 0.02	91.6 ± 2.3	1356.2 ± 1.6	1588.8 ± 2.1
	individual particle C0002	intact part.	30	161.8 ± 8.9	0.66 ± 0.04	88.7 ± 12.4	1361.6 ± 7.9	1594.2 ± 4.1
		IOM	30	173.4 ± 4.4	0.71 ± 0.03	92.8 ± 3.1	1357.0 ± 2.4	1587.6 ± 2.0
	C0107_IOM residue	IOM*	38	174.7 ± 4.9	0.69 ± 0.02	92.7 ± 4.0	1356.1 ± 2.5	1587.6 ± 2.1

Spectral parameters ($FWHM_D$, I_D/I_G, $FWHM_G$, ω_D, ω_G) obtained through the reduction of "n" spectra – Sample type is either intact particle (intact part.) or Insoluble Organic Matter (IOM) either chemically extracted by H. Yabuta (PI of PET IOM) or * in Grenoble (see text for explanations).

et al., 2018). These spectral ranges were first tested on the Raman dataset obtained on Ryugu samples, but, a high rate of unsuccessful spectral fitting was resulting. The procedure was thus modified with a baseline correction performed between 1000 and 1700 cm^{-1}, leading to a successful fitting of each spectrum. The D- and G-bands on the spectra acquired on Ryugu samples are superimposed to a fluorescence background that tends to be, on average, of higher intensity than for type 2 chondrites (Fig. 3a). It is of the same range of order as for Orgueil (Fig. 3a), but the G-band on Orgueil spectra is better defined than on Ryugu samples. Moreover, with such a high fluorescence background, the edge filter of the instrument (532 nm RazorEdge® ultra steep long-pass edge filter, provided by the manufacturer Semrock and designed to be used as an ultra-wide and low-ripple passband edge filter for Raman spectroscopy) induces ripples on the measured spectra (Casadio et al., 2017; Alleon et al., 2021). This artifact induces a high-frequency sinusoidal signal, whose frequency decreases with increasing wavenumber. In this case, a weak Raman signal superimposed over an intrinsically high luminescence is difficult to identify without appropriate data processing for background subtraction. Altogether, these observations (high fluorescence, instrumentally-linked undulatory variation of the intensity, G-band less defined than in Orgueil) might explain why the Raman spectra acquired on the Ryugu samples were difficult to fit. The Raman spectra of chondrites considered as references for comparison of spectral parameters were subsequently mathematically adjusted along the exact same procedure as the Ryugu samples.

3.3. Raman spectra and spectral parameters of the Ryugu samples

Average Raman spectra obtained on fragments of individual particles and aggregates from Chamber A and Chamber C Ryugu samples (Bonal and Montagnac, 2021) are available online in the GhoSST/SSHADE spectral database.

The Raman spectra acquired on several fragments of each allocated Ryugu sample (Table 1) exhibit the so-called D- and G-band reflecting the systematic presence of polyaromatic carbonaceous matter. The Raman signature are superimposed on a high fluorescence background (Fig. 3). The origin of fluorescence in natural and complex samples can be multiple and related either to minerals or to organics. Nevertheless, based on dedicated fluorescence spectra measured on raw chondritic matrix and extracted chondritic IOM, it was previously suggested that for the type of samples we consider, fluorescence signal is induced by organic matter (Quirico et al., 2005). Still, some specific work to disentangle the respective contribution of poorly ordered carbonaceous matter and of small individual organic molecules referred to as "soluble organic matter" would be required. This is partly discussed in Komatsu et al. (2022) and Komatsu et al. (under revision).

Raman spectral parameters (average and standard deviations) computed from individual spectra acquired on Ryugu particles (intact particles and chemically extracted IOM) are reported in Table 3. Parameters obtained from reference chondrites are in supplementary material (Table A2).

4. Discussion

Chondritic samples (either collected on Earth as meteorites for example or in situ on a given asteroid) are primitive, but not pristine. They have been modified to variable extents by several processes on their original parent body(ies). In particular, thermal heating might have occurred on a relatively long timescale through radioactive decay of short-lived radionuclides such as ^{26}Al or on a much shorter timescale through the passage of a shock wave (see e.g. review by Huss et al. (2006)). In particular, effects of radioactive decay are visible in chondrites of petrologic type 3 and above. Type 1 and 2 chondrites basically escaped this long-term heating. Nevertheless, based on the study of 39 CM and C2-ungrouped chondrites, Quirico et al. (2018) showed that >35% of the samples had experienced some heating, most likely short-duration heating triggered by impacts. Quirico et al. (2018) proposed a carbon-based classification of heated C2 chondrites (identified as "R2" and "R3" samples as opposed to "R1" indicating unheated samples, see Section 4.2. for explanation), consistent with the classification

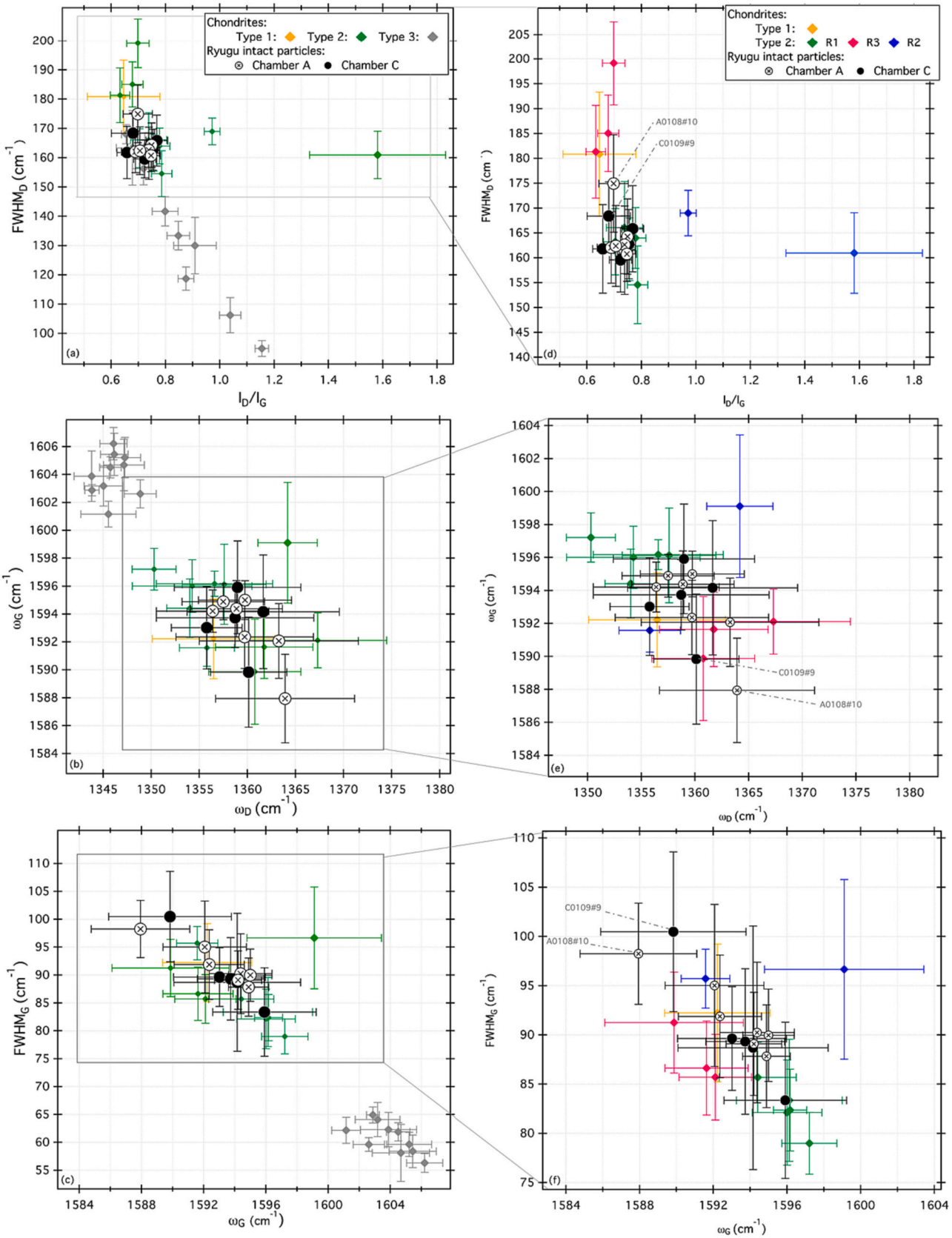

Fig. 4. Spectral parameters of Raman bands of carbonaceous materials ((a, d) $FWHM_D$ vs. I_D/I_G, (b, d) ω_G vs. ω_D, (c, f) $FWHM_G$ vs. ω_G) in the Ryugu intact particles (in black) as compared to reference chondrites (CI Orgueil in yellow, type 2 CM chondrites in green on Figs. a, b, c and in green, magenta and blue on Figs. d, e, f and type 3 chondrites in grey). The three colors for type 2 chondrites ("R1" in green, "R3" in magenta, and "R2" in blue) reflect variable extents of short-duration heating (see Section 4.2. for explanation and Quirico et al., 2018). Averages (symbols) and standard deviations (bars) are plotted for each sample. (For interpretation of the references to colour in this figure legend, the reader is referred to the web version of this article.)

developed by Nakamura (2005) based on mineralogical tracers.

The objectives here are *(i)* to understand whether or not the primordial planetesimal, from which Ryugu formed, accreted early enough or was large enough to have trapped sufficient radioactive elements leading to long-term metamorphism, and *(ii)* to unveil whether shock heating induced by potential impacts experienced by Ryugu might have been recorded in the samples collected by Hayabusa2.

4.1. Ryugu samples escaped significant long-term radioactive thermal metamorphism

The structural order of the polyaromatic carbonaceous matter present in primitive chondrites reflects the thermal history experienced by the whole rock (e.g., Bonal et al., 2016; Quirico et al., 2018). In particular, it is relatively straightforward to distinguish type 2 from type 3 chondrites based on a combination of Raman spectral parameters (Fig. 4a-c): on the graph $FWHM_D$ vs. I_D/I_G (Fig. 4a), there is a small overlap between the least metamorphosed type 3 chondrites and types 1 and 2 chondrites, but in the graphs $FWHM_G$ vs. ω_G (Fig. 4b) and ω_G vs. ω_D (Fig. 4c), types 1 and 2 chondrites are clearly plotting apart from type 3 chondrites.

The spectral parameters of the Ryugu intact particles are all plotting together in the area defined by types 1 and 2 chondrites. In particular, in the graphs $FWHM_G$ vs. ω_G (Fig. 4b) and ω_G vs. ω_D (Fig. 4c), spectral parameters from Hayabusa2 samples are clearly plotted in an area distinct from type 3 chondrites. This shows that the Ryugu particles considered in the present work and in Yabuta et al. (2023) escaped significant long-term radioactive heating. This is consistent with Raman measurements led by Nakamura E. et al. (2022), who showed that their Ryugu particles had spectral parameters comparable to Orgueil, Murchison and Murray (CM2).

4.2. Structural variability among the Ryugu intact samples

Fragments of 12 intact Ryugu particles were characterized by Raman spectroscopy (Table 3). Their respective average spectral parameters are all plotted among type 2 chondrites (see 4.1 part). There is no obvious systematic structural difference between Chamber A and Chamber C particles (Fig. 4a-c). A Student's *t*-test was previously used (Bonal et al., 2022) to evaluate the null hypothesis that the means of the spectral parameters from the particles characterized at that time – A0108 (−6, 10, 18) and C0109 (−5, 9, 12) – were equal. It was concluded that the polyaromatic structure of organic materials in the intact samples from A0108 and C0109 aggregates appeared to be slightly different (Bonal et al., 2022). However, since then *(i)* a better understanding of what are aggregates and *(ii)* higher statistics of measurements (by almost a factor 2) lead us to consider different null hypothesis to be evaluated through Student's t-test. As mentioned earlier, in the curation facility, individual particles (1–2 mm as typical dimensions) were picked out and the remaining mass was separated in several sets of aggregate samples. Aggregate samples consist of fine grains (mostly smaller than 1 mm) that were mixed within the sample chamber and were put together "artificially" on Earth as they were not necessarily present as aggregates on the surface of Ryugu before the touchdowns and collections. As such, there is no specific reason to consider that particles A0108–6, 10, 18 and 61 are representative of the bulk A0108 aggregate (and the same observation can be done for particles C0109–5, 9 and 12 and aggregate C0109). It seems more meaningful not to assume the particles of a given aggregates to have the same characteristics. On the other hand, the samples stored in Chamber A and Chamber C have been collected over two touchdowns in different places (Tsuda et al., 2020). Considering them separately and comparing their various characteristics – such as the structure of the polyaromatic carbonaceous matter – appears to be much more legitimate. We have thus tested the null hypothesis that the means of the spectral parameters from Chamber A and Chamber C are equal: the result of the test indicates that the mean value of $FWHM_D$, I_D/I_G, $FWHM_G$, ω_G and ω_D from all the Chamber A and Chamber C particles considered in the present work cannot be considered as distinct. We thus conclude that among the particles considered in the present work and in Yabuta et al. (2023) and collected from the surface (Chamber A) and surface and sub-surface (Chamber C) asteroid regolith, there is no systematic difference in the structural order of their polyaromatic carbonaceous matter. This is in contrast with Nakamura E. et al. (2022) who revealed differences in Raman parameters between Chamber A and Chamber C samples and interpreted them as indicative of a higher exposure to solar irradiation of the surface (vs. sub-surface).

Among type 2 chondrites, structural variability of the polyaromatic carbonaceous matter has been previously revealed and interpreted as reflecting short-duration heating most likely related to impacts (Quirico et al., 2018). In particular, three subgroups (R1, R2 and R3) were defined. R1 designates the structural order of most of the type 2 chondrites that are basically unheated (e.g., Murchison, Nogoya…). R3s exhibit some slight structural modifications in comparison to R1s and have most likely been moderately heated (e.g., WIS 91600, Cold Bokkeveld…). Lastly, R2s exhibit some substantial structural modifications in comparison to R1s: they have been heated (e.g., PCA 02012, PCA 91008). On the graph $FWHM_D$ vs. I_D/I_G (Figs. 4a and d), R2s are easily identified as they are plotting off the main trend with higher I_D/I_G and R3s are characterized by larger $FWHM_D$ than R1s. On $FWHM_G$ vs. ω_G (Figs. 4c and f), R3s and R2s are again slightly off the R1s with lower ω_G and higher $FWHM_G$, respectively. Moreover, ω_D tend to be at higher wavenumbers for R2s and R3s than for R1s (Figs. 4b-e). In terms of average spectra, the fluorescence background of R3s is not significatively different from R1s, but the G-band is narrower and the spectral valley between the D- and G-bands is deeper than on R1s spectra (Fig. 3a). The fluorescence background of R2s is significantly lower than in R1s and R3s (Fig. 3a). In a manner similar to type 2 chondrites, CI chondrites basically escaped significant heating. Under the hypothesis of a similar kinetics, structural order of the polyaromatic carbonaceous matter is sensitive to the peak temperature (e.g., Bonal et al., 2016). The temperature experienced by types 1 and 2 chondrites is not firmly established with estimations from 20 to 150 °C for CIs and from 0 to 80 °C for CMs (see review by Brearley, 2006). These overlapping ranges of temperatures are consistent with the absence of distinction between Orgueil and type 2 chondrites based on the structural order of their polyaromatic carbonaceous matter (Fig. 4d-f). Still, average Raman spectra of Orgueil is significantly more fluorescent than those of type 2 chondrites (Fig. 3a). To be noted, the acquisition of Raman spectra of Ivuna fragments has been attempted with the experimental conditions similar to all the other samples but was unsuccessful: the intensity of the fluorescence background was systematically higher than for Orgueil and led to the saturation of the instrument detector.

The majority of the Ryugu intact particles considered in the present work overlaps with unheated (R1) type 2 chondrites. Only A0108–10 and C0109–9 are plotted slightly apart R1s and towards R3s. Their average Raman spectra exhibit a fluorescence background *(i)* lower than the other Ryugu particles, but *(ii)* similar or higher than R1 type 2 chondrites (Fig. 3a). The easiest way to interpret the small structural variability observed among the Ryugu samples studied in the present work is to consider some very moderate heating experienced by the particle C0109–9 and particle A0108–10. This is consistent with the relatively high CH_2/CH_3 ratio of the IOM of A0108–10 as estimated from infrared spectra (Quirico et al., 2022 and corresponding paper Quirico et al., accepted). In addition, mineralogical and textural signatures of impact-driven heating in Ryugu grains as revealed by Noguchi et al. (2023) (in ~7% of analyzed samples) support the plausible presence of heated material within Ryugu's regolith. On the other hand, the IOM from C0109–9 is not characterized by a higher CH_2/CH_3 ratio. This apparent discrepancy might simply reflect a very moderate heating that did not lead to structural and chemical modifications homogeneously throughout the considered particle (i.e., the fragments used for chemical extraction being different from the one characterized by Raman

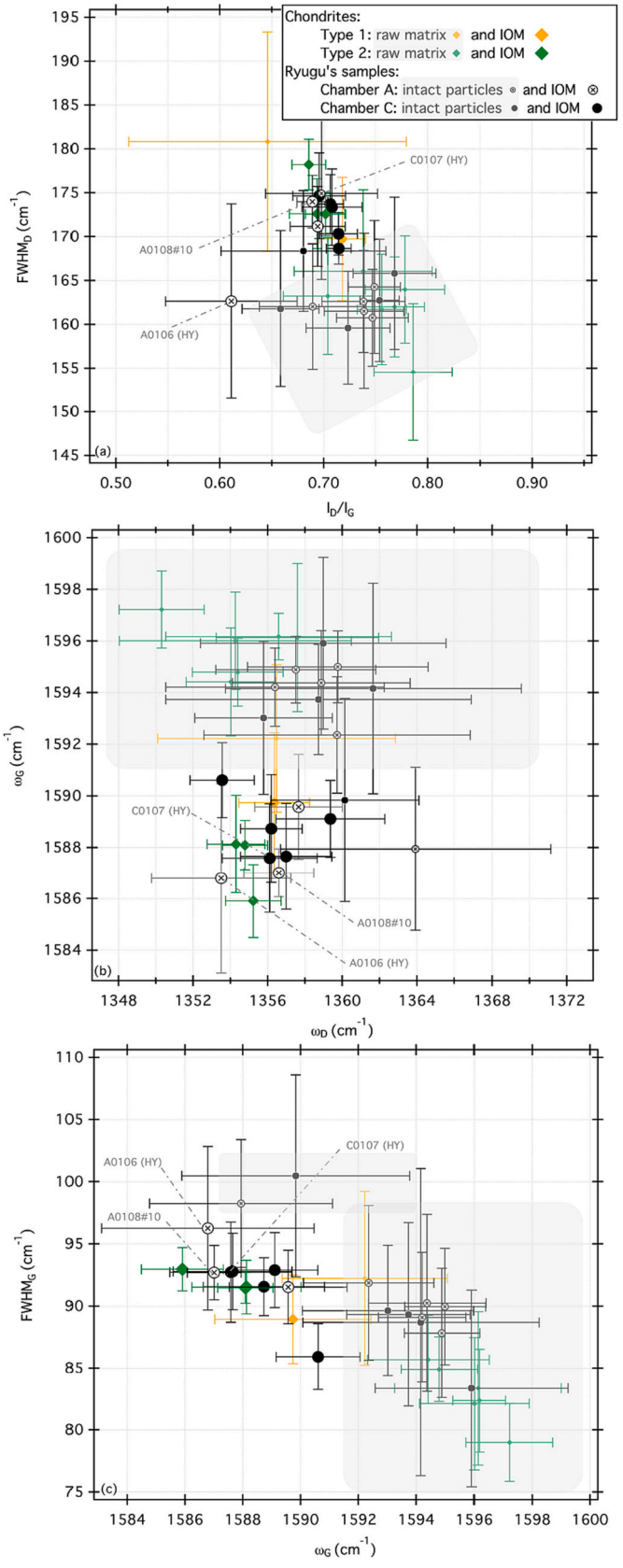

(caption on next column)

Fig. 5. Spectral parameters of Raman bands ((a) $FWHM_D$ vs. I_D/I_G, (b) ω_G vs. ω_D, (c) $FWHM_G$ vs. ω_G) obtained on IOM chemically extracted from Hayabusa2 particles (in black) and reference chondrites (type 1 CI Orgueil in yellow and type 2 CM chondrites (R1) in green). For comparison, corresponding data for intact particles and matrix fragments are reported and shaded in grey. Most of the IOM were chemically extracted at IPAG, except two of them that were extracted by H. Yabuta (HY on the graph). Averages (symbols) and standard deviations (bars) are plotted for each sample. (For interpretation of the references to colour in this figure legend, the reader is referred to the web version of this article.)

spectroscopy).

Very moderate heating appears to be the easiest way to explain the organic structural variability revealed by the present Raman measurements. Nevertheless, the possibility of distinct organic precursors might not be actually totally ruled out: *(i)* Ryugu's regolith could indeed have been bombarded by micrometeorites; and *(ii)* the brecciated nature of some coarse samples has recently been revealed (Nakamura T. et al., 2023). However, investigating such a possibility requires a combined characterization of organics and mineralogy in a considered petrographic context. This approach was not possible in the timeframe of the Hayabusa 2 initial Analysis. Moreover, the similarity of organic precursors among primitive chondrites is usually hypothesized and appears as the simplest and most appropriate approach so far (e.g., Alexander et al., 2017).

4.3. IOM

Raman spectra acquired on the chemically extracted IOM also systematically exhibit, unsurprisingly, the D- and G-bands related to the presence of polyaromatic carbonaceous matter (Fig. 3b). The intensity of the fluorescence background is noticeably lower (Fig. 3a) than on the spectra obtained on intact matrix fragments and intact Ryugu particles (Fig. 3b), with the exception of the IOM extracted on bulk aggregates A0106 (HY) and C0107 (HY) (Fig. 3b). On the graph $FWHM_D$ vs. I_D/I_G (Fig. 5a), AO106 (HY) appears to be slightly off the area defined by the other IOMs (from the Ryugu samples and type 2 chondrites). However, taking into account the standard deviation of each other spectral parameter (Fig. 5b-c), there is no systematic difference between IOMs A0106 (HY) and C0107 (HY) and the others. The derived spectral parameters are shifted in comparison to parameters obtained on intact matrix fragments and Ryugu intact particles (Fig. 5). These differences could be related to the absence of the so-called soluble organic matter, but a different sensitivity to the incident laser could also play a role. Understanding precisely the influence of the extraction on spectral difference between IOM and intact samples would need a dedicated investigation (e.g., Kebukawa et al., 2019), that is behind the scope of the present paper. Nevertheless, one notes that the spectral parameters relative to Ryugu particles are superimposed with those of types 1 and 2 chondrites. This is consistent with the fact that these Ryugu particles escaped significant heating (see part 4.1). No IOM of slightly heated type 2 chondrites (R2, R3, see part 4.2) has been obtained and characterized in the timeframe of the initial analysis. As such, a precise characterization of the short-duration thermal history potentially experienced by Ryugu is not possible based on IOM. However, the IOM extracted from particle A0108–10 does not appear to be characterized by spectral parameters distinguishable from the other particles or reference chondrites (Fig. 5). This again shows that if A0108–10 indeed experienced some heating to explain the spectral parameters of the intact particles, it was very moderate.

5. Conclusion

The main conclusions based on the interpretation of the Raman spectral data acquired on a series of 11 Ryugu intact particles and 8 extracted IOM are the following:

- There is no structural difference of the polyaromatic component probed by Raman spectroscopy between Chamber A and Chamber C particles
- In a manner similar to type 1 and 2 chondrites, the characterized Ryugu particles did not experience significant long-duration thermal metamorphism related to the radioactive decay of elements such as ^{26}Al
- Some structural variability is nevertheless observed within our particle set. It may be interpreted as some particles having experienced some short-duration and weak heating (R3 in the scale defined by Quirico et al., 2018 and TII or lower according to the scale defined by Nakamura, 2005), in a manner similar to primitive carbonaceous chondrites.

Raman spectroscopy provides the maturation grade of the polyaromatic carbonaceous matter, and finally its degree of heating as a result of the time–temperature history. Three types of heating processes can be considered: collisional, solar, and radiogenic. The latter one is not compatible with the structural order of the polyaromatic carbonaceous matter observed in the considered Hayabusa2 samples. The surface of Ryugu has been subjected to high temperature (e.g., Kitazato et al., 2021) that could induced some structural modification of the carbonaceous matter. But still we do favor a collisional origin for the observed structural heterogeneity as it is compatible with the idea that "Ryugu is the product of more than one generation of parent body disruption"as proposed by Morota et al. (2020). This is also consistent with sparse zolenskyite identified in some Ryugu particles (Tomioka et al., 2023) – this high-pressure phase of daubreelite being formed at a few gigapascals (Ma and Rubin, 2022). Some rare evidences of shock (compression axis, sets of fractures) have also been recently reported by Nakamura E. et al. (2022) and Nakamura T. et al. (2023) in one out of seventeen particles. The main conclusions that Ryugu escaped significant long-duration thermal metamorphism and exhibits only a few evidences of shocks at high pressure and/or high temperature are consistent with the mineralogy (i.e., fine-grained materials of phyllosilicate minerals) of the Ryugu samples (e.g., Nakamura E. et al., 2022; Nakamura T. et al., 2023; Yokoyama et al., 2022). This is also consistent, for example, with *(i)* the chemical, isotopic, and morphological diversities of macromolecular organic matter interpreted as recording various degrees of parent body aqueous alteration (Yabuta et al., 2023), *(ii)* the molecular diversity revealed in SOM (Naraoka et al., 2023), *(iii)* the elemental and isotopic compositions of IOM (Remusat et al., 2022), *(iv)* the abundance and variety of presolar grains (Barosch et al., 2022), (*v*) planetary noble gas concentrations equivalent to or even higher than CI chondrites (Okazaki et al., 2022). Lastly, this is consistent with the similarity established between Ryugu samples and CI chondrites (Yokoyama et al., 2022).

Declaration of Competing Interest

The authors declare that they have no known competing financial interests or personal relationships that could have appeared to influence the work reported in this paper.

Data availability

The spectral data will be made available on the SSHADE/GhoSST database once the paper is accepted.

Acknowledgments

This research was supported by grant from the French spatial agency CNES (Centre National d'Etudes Spatiales). The Raman facility in Lyon (France) is supported by the Institut National des Sciences de l'Univers (INSU). It is a contribution of the LabEx Lyon Institute of Origins (ANR-10-LABX-0066), within the program "Investissements d'Avenir" (ANR-11-IDEX-0007) at Université de Lyon.

Appendix A. Supplementary data

Supplementary data to this article can be found online at https://doi.org/10.1016/j.icarus.2023.115826.

References

Alexander, C.M.O.D., Cody, G.D., De Gregorio, B.T., Nittler, L.R., Stroud, R.M., 2017. The nature, origin and modification of insoluble organic matter in chondrites, the major source of Earth's C and N. Chem. Erde-Geochem. 77, 227–256. https://doi.org/10.1016/j.chemer.2017.01.007.

Alleon, J., Montagnac, G., Reynard, B., Brulé, T., Thoury, M., Gueriau, P., 2021. Pushing Raman spectroscopy over the edge: purported signatures of organic molecules in fossil animals are instrumental artefacts. BioEssays 43, 2000295. https://doi.org/10.1002/bies.202000295.

Arakawa, M., Saiki, T., Wada, K., Ogawa, K., Kadono, T., Shirai, K., Sawada, H., Ishibashi, K., Honda, R., Sakatani, N., Iijima, Y., Okamoto, C., Yano, H., Takagi, Y., Hayakawa, M., Michel, P., Jutzi, M., Shimaki, Y., Kimura, S., Mimasu, Y., Toda, T., Imamura, H., Nakazawa, S., Hayakawa, H., Sugita, S., Morota, T., Kameda, S., Tatsumi, E., Cho, Y., Yoshioka, K., Yokota, Y., Matsuoka, M., Yamada, M., Kouyama, T., Honda, C., Tsuda, Y., Watanabe, S., Yoshikawa, M., Tanaka, S., Terui, F., Kikuchi, S., Yamaguchi, T., Ogawa, N., Ono, G., Yoshikawa, K., Takahashi, T., Takei, Y., Fujii, A., Takeuchi, H., Yamamoto, Y., Okada, T., Hirose, C., Hosoda, S., Mori, O., Shimada, T., Soldini, S., Tsukizaki, R., Iwata, T., Ozaki, M., Abe, M., Namiki, N., Kitazato, K., Tachibana, S., Ikeda, H., Hirata, N., Hirata, N., Noguchi, R., Miura, A., 2020. An artificial impact on the asteroid (162173) Ryugu formed a crater in the gravity-dominated regime. Science 368, 67–71. https://doi.org/10.1126/science.aaz1701.

Barosch, J., Nittler, L.R., Wang, J., Alexander, C.M.O., De Gregorio, B.T., Engrand, C., Kebukawa, Y., Nagashima, K., Stroud, R.M., Yabuta, H., Abe, Y., Aléon, J., Amari, S., Amelin, Y., Bajo, K., Bejach, L., Bizzarro, M., Bonal, L., Bouvier, A., Carlson, R.W., Chaussidon, M., Choi, B.-G., Cody, G.D., Dartois, E., Dauphas, N., Davis, A.M., Dazzi, A., Deniset-Besseau, A., Di Rocco, T., Duprat, J., Fujiya, W., Fukai, R., Gautam, I., Haba, M.K., Hashiguchi, M., Hibiya, Y., Hidaka, H., Homma, H., Hoppe, P., Huss, G.R., Ichida, K., Iizuka, T., Ireland, T.R., Ishikawa, A., Ito, M., Itoh, S., Kamide, K., Kawasaki, N., David Kilcoyne, A.L., Kita, N.T., Kitajima, K., Kleine, T., Komatani, S., Komatsu, M., Krot, A.N., Liu, M.-C., Martins, Z., Masuda, Y., Mathurin, J., McKeegan, K.D., Montagnac, G., Morita, M., Mostefaoui, S., Motomura, K., Moynier, F., Nakai, I., Nguyen, A.N., Ohigashi, T., Okumura, T., Onose, M., Pack, A., Park, C., Piani, L., Qin, L., Quirico, E., Remusat, L., Russell, S.S., Sakamoto, N., Sandford, S.A., Schönbächler, M., Shigenaka, M., Suga, H., Tafla, L., Takahashi, Y., Takeichi, Y., Tamenori, Y., Tang, H., Terada, K., Terada, Y., Usui, T., Verdier-Paoletti, M., Wada, S., Wadhwa, M., Wakabayashi, D., Walker, R.J., Yamashita, K., Yamashita, S., Yin, Q.-Z., Yokoyama, T., Yoneda, S., Young, E.D., Yui, H., Zhang, A.-C., Abe, M., Miyazaki, A., Nakato, A., Nakazawa, S., Nishimura, M., Okada, T., Saiki, T., Tanaka, S., Terui, F., Tsuda, Y., Watanabe, S., Yada, T., Yogata, K., Yoshikawa, M., Nakamura, T., Naraoka, H., Noguchi, T., Okazaki, R., Sakamoto, K., Tachibana, S., Yurimoto, H., 2022. Presolar stardust in asteroid Ryugu. Astrophys. J. 935, L3. https://doi.org/10.3847/2041-8213/ac83bd.

Battandier, M., Bonal, L., Quirico, E., Beck, P., Engrand, C., Duprat, J., Dartois, E., 2018. Characterization of the organic matter and hydration state of Antarctic micrometeorites: a reservoir distinct from carbonaceous chondrites. Icarus 306, 74–93. https://doi.org/10.1016/j.icarus.2018.02.002.

Bonal, L., Montagnac, G., 2021. Average Raman spectra (λ = 532 nm) obtained on fragments of individual particles and aggregates from Chamber A and Chamber C Ryugu samples (Hayabusa2 mission). SSHADE/GhoSST (OSUG Data Center). Dataset/Spectral Data. https://doi.org/10.26302/SSHADE/EXPERIMENT_LB_20221102_001.

Bonal, L., Quirico, E., Bourot-Denise, M., Montagnac, G., 2006. Determination of the petrologic type of CV3 chondrites by Raman spectroscopy of included organic matter. Geochim. Cosmochim. Acta 70, 1849–1863. https://doi.org/10.1016/j.gca.2005.12.004.

Bonal, L., Quirico, E., Flandinet, L., Montagnac, G., 2016. Thermal history of type 3 chondrites from the Antarctic meteorite collection determined by Raman spectroscopy of their polyaromatic carbonaceous matter. Geochim. Cosmochim. Acta 189, 312–337. https://doi.org/10.1016/j.gca.2016.06.017.

Bonal, L., Quirico, E., Montagnac, G., Komatsu, M., Yabuta, H., Yurimoto, H., Nakamura, T., Noguchi, T., Okazaki, R., Naraoka, H., Sakamoto, K., Tachibana, S., Watanabe, S., Tsuda, Y., Hayabusa2-Initial-Analysis IOM Team, 2022. Thermal History of Ryugu Based on Raman Characterization of Hayabusa2 Samples 53rd Lunar and Planetary Science Conference, held 7–11 March, 2022 at The Woodlands, Texas. LPI Contribution No. 2678, 2022, id.1331.

Brearley, A.J., 2006. The action of water. In: Lauretta, D.S., McSween Jr., H.Y. (Eds.), Meteorites and the Early Solar System II. Tucson, pp. 584–624.

Busemann, H., Alexander, M.O., Nittler, L.R., 2007. Characterization of insoluble organic matter in primitive meteorites by microRaman spectroscopy. Meteorit. Planet. Sci. 42, 1387–1416. https://doi.org/10.1111/j.1945-5100.2007.tb00581.x.

Casadio, F., Daher, C., Bellot-Gurlet, L., 2017. Raman spectroscopy of cultural heritage materials: overview of applications and new Frontiers in instrumentation, sampling modalities, and data processing. In: Mazzeo, R. (Ed.), Analytical Chemistry for

Cultural Heritage, Topics in Current Chemistry Collections. Springer International Publishing, Cham, pp. 161–211. https://doi.org/10.1007/978-3-319-52804-5_5.
DeMeo, F.E., Carry, B., 2013. The taxonomic distribution of asteroids from multi-filter all-sky photometric surveys. Icarus 226, 723–741. https://doi.org/10.1016/j.icarus.2013.06.027.
DeMeo, F.E., Carry, B., 2014. Solar system evolution from compositional mapping of the asteroid belt. Nature 505, 629–634. https://doi.org/10.1038/nature12908.
DeMeo, F.E., Alexander, C.M.O., Walsh, K.J., Chapman, C.R., Binzel, R.P., 2015. The compositional structure of the asteroid belt. Asteroids IV. https://doi.org/10.2458/azu_uapress_9780816532131-ch002.
Dobrică, E., Engrand, C., Quirico, E., Montagnac, G., Duprat, J., 2011. Raman characterization of carbonaceous matter in CONCORDIA Antarctic micrometeorites: Raman characterization of carbonaceous matter in micrometeorites. Meteorit. Planet. Sci. 46, 1363–1375. https://doi.org/10.1111/j.1945-5100.2011.01235.x.
Ferrari, A., Robertson, J., 2000. Interpretation of Raman spectra of disordered and amorphous carbon. Phys. Rev. B - Conden. Matter Mater. Phys. 61, 14095–14107. https://doi.org/10.1103/PhysRevB.61.14095.
Ho, T.-M., Jaumann, R., Bibring, J.-P., Grott, M., Glaßmeier, K.-H., Moussi, A., Krause, C., Auster, U., Baturkin, V., Biele, J., Cordero, F., Cozzoni, B., Dudal, C., Fantinati, C., Grimm, C., Grundmann, J.-T., Hamm, M., Herčik, D., Kayal, K., Knollenberg, J., Küchemann, O., Ksenik, E., Lange, C., Lange, M., Lorda, L., Maibaum, M., Mimasu, Y., Cenac-Morthe, C., Okada, T., Otto, K., Pilorget, C., Reill, J., Saiki, T., Sasaki, K., Schlotterer, M., Schmitz, N., Schröder, S., Termtanasombat, N., Toth, N., Tsuda, Y., Ulamec, S., Wolff, F., Yoshimitsu, T., Ziach, C., 2021. The MASCOT lander aboard Hayabusa2: the in-situ exploration of NEA (162173) Ryugu. Planet. Space Sci. 200, 105200 https://doi.org/10.1016/j.pss.2021.105200.
Huss, G.R., Rubin, A.E., Grossman, J.N., 2006. Thermal metamorphism in chondrites. In: Lauretta, D.S., McSween Jr., H.Y. (Eds.), Meteorites and the Early Solar System II. Tucson, pp. 567–586.
Kebukawa, Y., Alexander, C.M.O., Cody, G.D., 2019. Comparison of FT-IR spectra of bulk and acid insoluble organic matter in chondritic meteorites: an implication for missing carbon during demineralization. Meteorit. Planet. Sci. 54 (7), 1632–1641. https://doi.org/10.1111/maps.13302.
Kitazato, K., Milliken, R.E., Iwata, T., Abe, M., Ohtake, M., Matsuura, S., Takagi, Y., Nakamura, T., Hiroi, T., Matsuoka, M., Riu, L., Nakauchi, Y., Tsumura, K., Arai, T., Senshu, H., Hirata, N., Barucci, M.A., Brunetto, R., Pilorget, C., Poulet, F., Bibring, J.-P., Domingue, D.L., Vilas, F., Takir, D., Palomba, E., Galiano, A., Perna, D., Osawa, T., Komatsu, M., Nakato, A., Arai, T., Takato, N., Matsunaga, T., Arakawa, M., Saiki, T., Wada, K., Kadono, T., Imamura, H., Yano, H., Shirai, K., Hayakawa, M., Okamoto, C., Sawada, H., Ogawa, K., Iijima, Y., Sugita, S., Honda, R., Morota, T., Kameda, S., Tatsumi, E., Cho, Y., Yoshioka, K., Yokota, Y., Sakatani, N., Yamada, M., Kouyama, T., Suzuki, H., Honda, C., Namiki, N., Mizuno, T., Matsumoto, K., Noda, H., Ishihara, Y., Yamada, R., Yamamoto, K., Yoshida, F., Abe, S., Higuchi, A., Yamamoto, Y., Okada, T., Shimaki, Y., Noguchi, R., Miura, A., Hirata, N., Tachibana, S., Yabuta, H., Ishiguro, M., Ikeda, H., Takeuchi, H., Shimada, T., Mori, O., Hosoda, S., Tsukizaki, R., Soldini, S., Ozaki, M., Terui, F., Ogawa, N., Mimasu, Y., Ono, G., Yoshikawa, K., Hirose, C., Fujii, A., Takahashi, T., Kikuchi, S., Takei, Y., Yamaguchi, T., Nakazawa, S., Tanaka, S., Yoshikawa, M., Watanabe, S., Tsuda, Y., 2021. Thermally altered subsurface material of asteroid (162173) Ryugu. Nat. Astron. 1–5 https://doi.org/10.1038/s41550-020-01271-2.
Komatsu M. et al. (under revision) Investigation of carbon structure and fluorescence background characteritics of Ryugu particles and their extracted residues by Raman spectroscopy. MAPS.
Komatsu, M., Yabuta, H., Kebukawa, Y., Bonal, L., Quirico, E., Yurimoto, H., Nakamura, T., Noguchi, T., Okazaki, R., Naraoka, H., Sakamoto, K., Tachibana, S., Watanabe, S., Tsuda, Y., Hayabusa2-Initial-Analysis IOM Team, 2022. The Laser-Induced Fluorescence from Ryugu Particles and Their Extracted Residues by Raman Spectroscopy 53rd Lunar and Planetary Science Conference, Held 7–11 March, 2022 at The Woodlands, Texas. LPI Contribution No. 2678, 2022, id.1679.
Lespade, P., Marchand, A., Couzi, M., Cruege, F., 1984. Caracterisation de materiaux carbones par microspectrometrie Raman. Carbon 22, 375–385. https://doi.org/10.1016/0008-6223(84)90009-5.
Ma, C., Rubin, A.E., 2022. Zolenskyite, FeCr2S4, a new sulfide mineral from the Indarch meteorite. Am. Mineral. 107, 1030–1033. https://doi.org/10.2138/am-2022-8094.
Matthews, M.J., Pimenta, M.A., Dresselhaus, G., Dresselhaus, M.S., Endo, M., 1999. Origin of dispersive effects of the Raman D band in carbon materials. Phys. Rev. B 59, R6585–R6588. https://doi.org/10.1103/PhysRevB.59.R6585.
Morota, T., Sugita, S., Cho, Y., Kanamaru, M., Tatsumi, E., Sakatani, N., Honda, R., Hirata, N., Kikuchi, H., Yamada, M., Yokota, Y., Kameda, S., Matsuoka, M., Sawada, H., Honda, C., Kouyama, T., Ogawa, K., Suzuki, H., Yoshioka, K., Hayakawa, M., Hirata, N., Hirabayashi, M., Miyamoto, H., Michikami, T., Hiroi, T., Hemmi, R., Barnouin, O.S., Ernst, C.M., Kitazato, K., Nakamura, T., Riu, L., Senshu, H., Kobayashi, H., Sasaki, S., Komatsu, G., Tanabe, N., Fujii, Y., Irie, T., Suemitsu, M., Takaki, N., Sugimoto, C., Yumoto, K., Ishida, M., Kato, H., Moroi, K., Domingue, D., Michel, P., Pilorget, C., Iwata, T., Abe, M., Ohtake, M., Nakauchi, Y., Tsumura, K., Yabuta, H., Ishihara, Y., Noguchi, R., Matsumoto, K., Miura, A., Namiki, N., Tachibana, S., Arakawa, M., Ikeda, H., Wada, K., Mizuno, T., Hirose, C., Hosoda, S., Mori, O., Shimada, T., Soldini, S., Tsukizaki, R., Yano, H., Ozaki, M., Takeuchi, H., Yamamoto, Y., Okada, T., Shimaki, Y., Shirai, K., Iijima, Y., Noda, H., Kikuchi, S., Yamaguchi, T., Ogawa, N., Ono, G., Mimasu, Y., Yoshikawa, K., Takahashi, T., Takei, Y., Fujii, A., Nakazawa, S., Terui, F., Tanaka, S., Yoshikawa, M., Saiki, T., Watanabe, S., Tsuda, Y., 2020. Sample collection from asteroid (162173) Ryugu by Hayabusa2: implications for surface evolution. Science 368, 654–659. https://doi.org/10.1126/science.aaz6306.
Nakamura, T., 2005. Post-hydration thermal metamorphism of carbonaceous chondrites. J. Mineral. Petrol. Sci. 100, 260–272. https://doi.org/10.2465/jmps.100.260.
Nakamura, E., Kobayashi, K., Tanaka, R., Kunihiro, T., Kitagawa, H., Potiszil, C., Ota, T., Sakaguchi, C., Yamanaka, M., Ratnayake, D.M., Tripathi, H., Kumar, R., Avramescu, M.-L., Tsuchida, H., Yachi, Y., Miura, H., Abe, M., Fukai, R., Furuya, S., Hatakeda, K., Hayashi, T., Hitomi, Y., Kumagai, K., Miyazaki, A., Nakato, A., Nishimura, M., Okada, T., Soejima, H., Sugita, S., Suzuki, A., Usui, T., Yada, T., Yamamoto, D., Yogata, K., Yoshitake, M., Arakawa, M., Fujii, A., Hayakawa, M., Hirata, Naoyuki, Hirata, Naru, Honda, R., Honda, C., Hosoda, S., Iijima, Y., Ikeda, H., Ishiguro, M., Ishihara, Y., Iwata, T., Kawahara, K., Kikuchi, S., Kitazato, K., Matsumoto, K., Matsuoka, M., Michikami, T., Mimasu, Y., Miura, A., Morota, T., Nakazawa, S., Namiki, N., Noda, H., Noguchi, R., Ogawa, N., Ogawa, K., Okamoto, C., Ono, G., Ozaki, M., Saiki, T., Sakatani, N., Sawada, H., Senshu, H., Shimaki, Y., Shirai, K., Takei, Y., Takeuchi, H., Tanaka, S., Tatsumi, E., Terui, F., Tsukizaki, R., Wada, K., Yamada, M., Yamada, T., Yamamoto, Y., Yano, H., Yokota, Y., Yoshihara, K., Yoshikawa, M., Yoshikawa, K., Fujimoto, M., Watanabe, S., Tsuda, Y., 2022. On the origin and evolution of the asteroid Ryugu: a comprehensive geochemical perspective. Proc. Jpn. Acad. Ser. B 98, 227–282. https://doi.org/10.2183/pjab.98.015.
Nakamura, T., Matsumoto, M., Amano, K., Enokido, Y., Zolensky, M.E., Mikouchi, T., Genda, H., Tanaka, S., Zolotov, M.Y., Kurosawa, K., Wakita, S., Hyodo, R., Nagano, H., Nakashima, D., Takahashi, Y., Fujioka, Y., Kikuiri, M., Kagawa, E., Matsuoka, M., Brearley, A.J., Tsuchiyama, A., Uesugi, M., Matsuno, J., Kimura, Y., Sato, M., Milliken, R.E., Tatsumi, E., Sugita, S., Hiroi, T., Kitazato, K., Brownlee, D., Joswiak, D.J., Takahashi, M., Ninomiya, K., Takahashi, T., Osawa, T., Terada, K., Brenker, F.E., Tkalcec, B.J., Vincze, L., Brunetto, R., Aléon-Toppani, A., Chan, Q.H. S., Roskosz, M., Viennet, J.-C., Beck, P., Alp, E.E., Michikami, T., Nagaashi, Y., Tsuji, T., Ino, Y., Martinez, J., Han, J., Dolocan, A., Bodnar, R.J., Tanaka, M., Yoshida, H., Sugiyama, K., King, A.J., Fukushi, K., Suga, H., Yamashita, S., Kawai, T., Inoue, K., Nakato, A., Noguchi, T., Vilas, F., Hendrix, A.R., Jaramillo-Correa, C., Domingue, D.L., Dominguez, G., Gainsforth, Z., Engrand, C., Duprat, J., Russell, S.S., Bonato, E., Ma, C., Kawamoto, T., Wada, T., Watanabe, S., Endo, R., Enju, S., Riu, L., Rubino, S., Tack, P., Takeshita, S., Takeichi, Y., Takeuchi, A., Takigawa, A., Takir, D., Tanigaki, T., Taniguchi, A., Tsukamoto, K., Yagi, T., Yamada, S., Yamamoto, K., Yamashita, Y., Yasutake, M., Uesugi, K., Umegaki, I., Chiu, I., Ishizaki, T., Okumura, S., Palomba, E., Pilorget, C., Potin, S.M., Alasli, A., Anada, S., Araki, Y., Sakatani, N., Schultz, C., Sekizawa, O., Sitzman, S.D., Sugiura, K., Sun, M., Dartois, E., De Pauw, E., Dionnet, Z., Djouadi, Z., Falkenberg, G., Fujita, R., Fukuma, T., Gearba, I.R., Hagiya, K., Hu, M.Y., Kato, T., Kawamura, T., Kimura, M., Kubo, M.K., Langenhorst, F., Lantz, C., Lavina, B., Lindner, M., Zhao, J., Vekemans, B., Baklouti, D., Bazi, B., Borondics, F., Nagasawa, S., Nishiyama, G., Nitta, K., Mathurin, J., Matsumoto, T., Mitsukawa, I., Miura, H., Miyake, A., Miyake, Y., Yurimoto, H., Okazaki, R., Yabuta, H., Naraoka, H., Sakamoto, K., Tachibana, S., Connolly, H.C., Lauretta, D.S., Yoshitake, M., Yoshikawa, M., Yoshikawa, K., Yoshihara, K., Yokota, Y., Yogata, K., Yano, H., Yamamoto, Y., Yamamoto, D., Yamada, M., Yamada, T., Yada, T., Wada, K., Usui, T., Tsukizaki, R., Terui, F., Takeuchi, H., Takei, Y., Iwamae, A., Soejima, H., Shirai, K., Shimaki, Y., Senshu, H., Sawada, H., Saiki, T., Ozaki, M., Ono, G., Okada, T., Ogawa, N., Ogawa, K., Noguchi, R., Noda, H., Nishimura, M., Namiki, N., Nakazawa, S., Morota, T., Miyazaki, A., Miura, A., Mimasu, Y., Matsumoto, K., Kumagai, K., Kouyama, T., Kikuchi, S., Kawahara, K., Kameda, S., Iwata, T., Ishihara, Y., Ishiguro, M., Ikeda, H., Hosoda, S., Honda, R., Honda, C., Hitomi, Y., Hirata, N., Hirata, N., Hayashi, T., Hayakawa, M., Hatakeda, K., Furuya, S., Fukai, R., Fujii, A., Cho, Y., Arakawa, M., Abe, M., Watanabe, S., Tsuda, Y., 2023. Formation and evolution of carbonaceous asteroid Ryugu: direct evidence from returned samples. Science 379, eabn8671. https://doi.org/10.1126/science.abn8671.
Naraoka, H., Takano, Y., Dworkin, J.P., Oba, Y., Hamase, K., Furusho, A., Ogawa, N.O., Hashiguchi, M., Fukushima, K., Aoki, D., Schmitt-Kopplin, P., Aponte, J.C., Parker, E.T., Glavin, D.P., McLain, H.L., Elsila, J.E., Graham, H.V., Eiler, J.M., Orthous-Daunay, F.-R., Wolters, C., Isa, J., Vuitton, V., Thissen, R., Sakai, S., Yoshimura, T., Koga, T., Ohkouchi, N., Chikaraishi, Y., Sugahara, H., Mita, H., Furukawa, Y., Hertkorn, N., Ruf, A., Yurimoto, H., Nakamura, T., Noguchi, T., Okazaki, R., Yabuta, H., Sakamoto, K., Tachibana, S., Connolly, H.C., Lauretta, D.S., Abe, M., Yada, T., Nishimura, M., Yogata, K., Nakato, A., Yoshitake, M., Suzuki, A., Miyazaki, A., Furuya, S., Hatakeda, K., Soejima, H., Hitomi, Y., Kumagai, K., Usui, T., Hayashi, T., Yamamoto, D., Fukai, R., Kitazato, K., Sugita, S., Namiki, N., Arakawa, M., Ikeda, H., Ishiguro, M., Hirata, Naru, Wada, K., Ishihara, Y., Noguchi, R., Morota, T., Sakatani, N., Matsumoto, K., Senshu, H., Honda, R., Tatsumi, E., Yokota, Y., Honda, C., Michikami, T., Matsuoka, M., Miura, A., Noda, H., Yamada, T., Yoshihara, K., Kawahara, K., Ozaki, M., Iijima, Y., Yano, H., Hayakawa, M., Iwata, T., Tsukizaki, R., Sawada, H., Hosoda, S., Ogawa, K., Okamoto, C., Hirata, Naoyuki, Shirai, K., Shimaki, Y., Yamada, M., Okada, T., Yamamoto, Y., Takeuchi, H., Fujii, A., Takei, Y., Yoshikawa, K., Mimasu, Y., Ono, G., Ogawa, N., Kikuchi, S., Nakazawa, S., Terui, F., Tanaka, S., Saiki, T., Yoshikawa, M., Watanabe, S., Tsuda, Y., 2023. Soluble organic molecules in samples of the carbonaceous asteroid (162173) Ryugu. Science 379, eabn9033. https://doi.org/10.1126/science.abn9033.
Okazaki, R., Marty, B., Busemann, H., Hashizume, K., Gilmour, J.D., Meshik, A., Yada, T., Kitajima, F., Broadley, M.W., Byrne, D., Füri, E., Riebe, M.E.I., Krietsch, D., Maden, C., Ishida, A., Clay, P., Crowther, S.A., Fawcett, L., Lawton, T., Pravdivtseva, O., Miura, Y.N., Park, J., Bajo, K., Takano, Y., Yamada, K., Kawagucci, S., Matsui, Y., Yamamoto, M., Righter, K., Sakai, S., Iwata, N., Shirai, N., Sekimoto, S., Inagaki, M., Ebihara, M., Yokochi, R., Nishiizumi, K., Nagao, K., Lee, J. I., Kano, A., Caffee, M.W., Uemura, R., Nakamura, T., Naraoka, H., Noguchi, T., Yabuta, H., Yurimoto, H., Tachibana, S., Sawada, H., Sakamoto, K., Abe, M., Arakawa, M., Fujii, A., Hayakawa, M., Hirata, Naoyuki, Hirata, Naru, Honda, R., Honda, C., Hosoda, S., Iijima, Y., Ikeda, H., Ishiguro, M., Ishihara, Y., Iwata, T., Kawahara, K., Kikuchi, S., Kitazato, K., Matsumoto, K., Matsuoka, M., Michikami, T.,

Mimasu, Y., Miura, A., Morota, T., Nakazawa, S., Namiki, N., Noda, H., Noguchi, R., Ogawa, N., Ogawa, K., Okada, T., Okamoto, C., Ono, G., Ozaki, M., Saiki, T., Sakatani, N., Senshu, H., Shimaki, Y., Shirai, K., Sugita, S., Takei, Y., Takeuchi, H., Tanaka, S., Tatsumi, E., Terui, F., Tsukizaki, R., Wada, K., Yamada, M., Yamada, T., Yamamoto, Y., Yano, H., Yokota, Y., Yoshihara, K., Yoshikawa, M., Yoshikawa, K., Furuya, S., Hatakeda, K., Hayashi, T., Hitomi, Y., Kumagai, K., Miyazaki, A., Nakato, A., Nishimura, M., Soejima, H., Iwamae, A., Yamamoto, D., Yogata, K., Yoshitake, M., Fukai, R., Usui, T., Connolly, H.C., Lauretta, D., Watanabe, S., Tsuda, Y., 2022. Noble gases and nitrogen in samples of asteroid Ryugu record its volatile sources and recent surface evolution. Science 0, eabo0431. https://doi.org/10.1126/science.abo0431.

Pócsik, I., Hundhausen, M., Koós, M., Ley, L., 1998. Origin of the D peak in the Raman spectrum of microcrystalline graphite. J. Non-Cryst. Solids 227–230, 1083–1086. https://doi.org/10.1016/S0022-3093(98)00349-4.

Quirico, E., Rouzaud, J.-N., Bonal, L., Montagnac, G., 2005. Maturation grade of coals as revealed by Raman spectroscopy: progress and problems. In: Spectrochimica Acta Part a: Molecular and Biomolecular Spectroscopy, Georaman 2004: Sixth International Conference on Raman Spectroscopy Applied to the Earth and Planetary Sciences 61, pp. 2368–2377. https://doi.org/10.1016/j.saa.2005.02.015.

Quirico, E., Bonal, L., Beck, P., Alexander, C.M.O., Yabuta, H., Nakamura, T., Nakato, A., Flandinet, L., Montagnac, G., Schmitt-Kopplin, P., Herd, C.D.K., 2018. Prevalence and nature of heating processes in CM and C2-ungrouped chondrites as revealed by insoluble organic matter. Geochim. Cosmochim. Acta 241, 17–37. https://doi.org/10.1016/j.gca.2018.08.029.

Quirico, E., Bonal, L., Kebukawa, Y., Amano, K., Yabuta, H., Phan, V., Beck, P., Rémusat, L., Dartois, E., Engrand, C., Martins, Z., Bejach, L., Dazzi, A., Deniset-Besseau, A., Duprat, J., Mathurin, J., Montagnac, G., Barosch, J., Cody, G., De Gregorio, B., Enokido, Y., Hashiguchi, M., Kamide, K., Kilcoyne, D., Komatsu, M., Matsumoto, M., Mostefaoui, S., Nittler, L., Ohigashi, T., Okumura, T., Sandford, S., Shigenaka, M., Stroud, R., Suga, H., Takahashi, Y., Takeichi, Y., Tamenori, Y., Verdier-Paoletti, M., Wakabayashi, D., Nakamura, T., Naraoka, H., Noguchi, T., Okazaki, R., Yurimoto, H., Sakamoto, K., Tachibana, S., Watanabe, S., Yada, T., Nishimura, M., Nakato, A., Miyazaki, A., Yogata, K., Abe, M., Okada, T., Usui, T., Yoshikawa, M., Saiki, T., Tanaka, S., Terui, F., Nakazawa, S. (accepted) Compositional heterogeneity of incoluble organic matter extracted from asteroid Ryugu samples. Accepted in MAPS.

Quirico, E., Bonal, L., Kebukawa, Y., Dartois, E., Engrand, C., Duprat, J., Bejach, L., Mathurin, J., Dazzi, A., Deniset-Besseau, A., Yabuta, H., Yurimoto, H., Nakamura, T., Noguchi, T., Okazaki, R., Naraoka, H., Sakamoto, K., Tachibana, S., Watanabe, S., Tsuda, Y., 2022. Abundance and Composition of Organics in Hayabusa2 Samples: Insights from Micro-FTIR Spectroscopy. 53rd Lunar and Planetary Science Conference, held 7-11 March, 2022 at The Woodlands, Texas. LPI Contribution No. 2678, 2022, id.1514.

Remusat, L., Verdier-Paoletti, M., Mostefaoui, S., Yabuta, H., Engrand, C., Yurimoto, H., Nakamura, T., Noguchi, T., Okazaki, R., Naraoka, H., Sakamoto, K., Watanabe, S., Tsuda, Y., Tachibana, S., Hayabusa2-Initial-Analysis IOM Team, 2022. H- and N-Isotope Distributions in the Insoluble Organic Matter of Ryugu Samples. 53rd Lunar and Planetary Science Conference, held 7–11 March, 2022 at The Woodlands, Texas. LPI Contribution No. 2678, 2022, id.1448.

Tomioka, N., Yamaguchi, A., Ito, M., Uesugi, M., Imae, N., Shirai, N., Ohigashi, T., Kimura, M., Liu, M.-C., Greenwood, R.C., Uesugi, K., Nakato, A., Yogata, K., Yuzawa, H., Kodama, Y., Hirahara, K., Sakurai, I., Okada, I., Karouji, Y., Okazaki, K., Kurosawa, K., Noguchi, T., Miyake, A., Miyahara, M., Seto, Y., Matsumoto, T., Igami, Y., Nakazawa, S., Okada, T., Saiki, T., Tanaka, S., Terui, F., Yoshikawa, M., Miyazaki, A., Nishimura, M., Yada, T., Abe, M., Usui, T., Watanabe, S., Tsuda, Y., 2023. A history of mild shocks experienced by the regolith particles on hydrated asteroid Ryugu. Nat Astron 1–9. https://doi.org/10.1038/s41550-023-01947-5.

Tsuda, Y., Saiki, T., Terui, F., Nakazawa, S., Yoshikawa, M., Watanabe, S., Hayabusa2 Project Team, 2020. Hayabusa2 mission status: landing, roving and cratering on asteroid Ryugu. Acta Astronaut. 171, 42–54. https://doi.org/10.1016/j.actaastro.2020.02.035.

Watanabe, S., Hirabayashi, M., Hirata, N., Hirata, Na, Noguchi, R., Shimaki, Y., Ikeda, H., Tatsumi, E., Yoshikawa, M., Kikuchi, S., Yabuta, H., Nakamura, T., Tachibana, S., Ishihara, Y., Morota, T., Kitazato, K., Sakatani, N., Matsumoto, K., Wada, K., Senshu, H., Honda, C., Michikami, T., Takeuchi, H., Kouyama, T., Honda, R., Kameda, S., Fuse, T., Miyamoto, H., Komatsu, G., Sugita, S., Okada, T., Namiki, N., Arakawa, M., Ishiguro, M., Abe, M., Gaskell, R., Palmer, E., Barnouin, O.S., Michel, P., French, A.S., McMahon, J.W., Scheeres, D.J., Abell, P.A., Yamamoto, Y., Tanaka, S., Shirai, K., Matsuoka, M., Yamada, M., Yokota, Y., Suzuki, H., Yoshioka, K., Cho, Y., Tanaka, S., Nishikawa, N., Sugiyama, T., Kikuchi, H., Hemmi, R., Yamaguchi, T., Ogawa, N., Ono, G., Mimasu, Y., Yoshikawa, K., Takahashi, T., Takei, Y., Fujii, A., Hirose, C., Iwata, T., Hayakawa, M., Hosoda, S., Mori, O., Sawada, H., Shimada, T., Soldini, S., Yano, H., Tsukizaki, R., Ozaki, M., Iijima, Y., Ogawa, K., Fujimoto, M., Ho, T.-M., Moussi, A., Jaumann, R., Bibring, J.-P., Krause, C., Terui, F., Saiki, T., Nakazawa, S., Tsuda, Y., 2019. Hayabusa2 arrives at the carbonaceous asteroid 162173 Ryugu—a spinning top-shaped rubble pile. Science 364, 268–272. https://doi.org/10.1126/science.aav8032.

Yabuta, H., Cody, G.D., Engrand, C., Kebukawa, Y., De Gregorio, B., Bonal, L., Remusat, L., Stroud, R., Quirico, E., Nittler, L., Hashiguchi, M., Komatsu, M., Okumura, T., Mathurin, J., Dartois, E., Duprat, J., Takahashi, Y., Takeichi, Y., Kilcoyne, D., Yamashita, S., Dazzi, A., Deniset-Besseau, A., Sandford, S., Martins, Z., Tamenori, Y., Ohigashi, T., Suga, H., Wakabayashi, D., Verdier-Paoletti, M., Mostefaoui, S., Montagnac, G., Barosch, J., Kamide, K., Shigenaka, M., Bejach, L., Matsumoto, M., Enokido, Y., Noguchi, T., Yurimoto, H., Nakamura, T., Okazaki, R., Naraoka, H., Sakamoto, K., Connolly, H.C., Lauretta, D.S., Abe, M., Okada, T., Yada, T., Nishimura, M., Yogata, K., Nakato, A., Yoshitake, M., Iwamae, A., Furuya, S., Hatakeda, K., Miyazaki, A., Soejima, H., Hitomi, Y., Kumagai, K., Usui, T., Hayashi, T., Yamamoto, D., Fukai, R., Sugita, S., Kitazato, K., Hirata, Naru, Honda, R., Morota, T., Tatsumi, E., Sakatani, N., Namiki, N., Matsumoto, K., Noguchi, R., Wada, K., Senshu, H., Ogawa, K., Yokota, Y., Ishihara, Y., Shimaki, Y., Yamada, M., Honda, C., Michikami, T., Matsuoka, M., Hirata, Naoyuki, Arakawa, M., Okamoto, C., Ishiguro, M., Jaumann, R., Bibring, J.-P., Grott, M., Schröder, S., Otto, K., Pilorget, C., Schmitz, N., Biele, J., Ho, T.-M., Moussi-Soffys, A., Miura, A., Noda, H., Yamada, T., Yoshihara, K., Kawahara, K., Ikeda, H., Yamamoto, Y., Shirai, K., Kikuchi, S., Ogawa, N., Takeuchi, H., Ono, G., Mimasu, Y., Yoshikawa, K., Takei, Y., Fujii, A., Iijima, Y., Nakazawa, S., Hosoda, S., Iwata, T., Hayakawa, M., Sawada, H., Yano, H., Tsukizaki, R., Ozaki, M., Terui, F., Tanaka, S., Fujimoto, M., Yoshikawa, M., Saiki, T., Tachibana, S., Watanabe, S., Tsuda, Y., 2023. Macromolecular organic matter in samples of the asteroid (162173) Ryugu. Science 379, eabn9057. https://doi.org/10.1126/science.abn9057.

Yada, T., Abe, M., Okada, T., Nakato, A., Yogata, K., Miyazaki, A., Hatakeda, K., Kumagai, K., Nishimura, M., Hitomi, Y., Soejima, H., Yoshitake, M., Iwamae, A., Furuya, S., Uesugi, M., Karouji, Y., Usui, T., Hayashi, T., Yamamoto, D., Fukai, R., Sugita, S., Cho, Y., Yumoto, K., Yabe, Y., Bibring, J.-P., Pilorget, C., Hamm, V., Brunetto, R., Riu, L., Lourit, L., Loizeau, D., Lequertier, G., Moussi-Soffys, A., Tachibana, S., Sawada, H., Okazaki, R., Takano, Y., Sakamoto, K., Miura, Y.N., Yano, H., Ireland, T.R., Yamada, T., Fujimoto, M., Kitazato, K., Namiki, N., Arakawa, M., Hirata, Naru, Yurimoto, H., Nakamura, T., Noguchi, T., Yabuta, H., Naraoka, H., Ito, M., Nakamura, E., Uesugi, K., Kobayashi, K., Michikami, T., Kikuchi, H., Hirata, Naoyuki, Ishihara, Y., Matsumoto, K., Noda, H., Noguchi, R., Shimaki, Y., Shirai, K., Ogawa, K., Wada, K., Senshu, H., Yamamoto, Y., Morota, T., Honda, R., Honda, C., Yokota, Y., Matsuoka, M., Sakatani, N., Tatsumi, E., Miura, A., Yamada, M., Fujii, A., Hirose, C., Hosoda, S., Ikeda, H., Iwata, T., Kikuchi, S., Mimasu, Y., Mori, O., Ogawa, N., Ono, G., Shimada, T., Soldini, S., Takahashi, T., Takei, Y., Takeuchi, H., Tsukizaki, R., Yoshikawa, K., Terui, F., Nakazawa, S., Tanaka, S., Saiki, T., Yoshikawa, M., Watanabe, S., Tsuda, Y., 2022. Preliminary analysis of the Hayabusa2 samples returned from C-type asteroid Ryugu. Nat. Astron. 6, 214–220. https://doi.org/10.1038/s41550-021-01550-6.

Yokoyama, T., Nagashima, K., Nakai, I., Young, E.D., Abe, Y., Aléon, J., Alexander, C.M.O., Amari, S., Amelin, Y., Bajo, K., Bizzarro, M., Bouvier, A., Carlson, R.W., Chaussidon, M., Choi, B.-G., Dauphas, N., Davis, A.M., Di Rocco, T., Fujiya, W., Fukai, R., Gautam, I., Haba, M.K., Hibiya, Y., Hidaka, H., Homma, H., Hoppe, P., Huss, G.R., Ichida, K., Iizuka, T., Ireland, T.R., Ishikawa, A., Ito, M., Itoh, S., Kawasaki, N., Kita, N.T., Kitajima, K., Kleine, T., Komatani, S., Krot, A.N., Liu, M.-C., Masuda, Y., McKeegan, K.D., Morita, M., Motomura, K., Moynier, F., Nguyen, A., Nittler, L., Onose, M., Pack, A., Park, C., Piani, L., Qin, L., Russell, S.S., Sakamoto, N., Schönbächler, M., Tafla, L., Tang, H., Terada, K., Terada, Y., Usui, T., Wada, S., Wadhwa, M., Walker, R.J., Yamashita, K., Yin, Q.-Z., Yoneda, S., Yui, H., Zhang, A.-C., Connolly, H.C., Lauretta, D.S., Nakamura, T., Naraoka, H., Noguchi, T., Okazaki, R., Sakamoto, K., Yabuta, H., Abe, M., Arakawa, M., Fujii, A., Hayakawa, M., Hirata, Naoyuki, Hirata, Naru, Honda, R., Honda, C., Hosoda, S., Iijima, Y., Ikeda, H., Ishiguro, M., Ishihara, Y., Iwata, T., Kawahara, K., Kikuchi, S., Kitazato, K., Matsumoto, K., Matsuoka, M., Michikami, T., Mimasu, Y., Miura, A., Morota, T., Nakazawa, S., Namiki, N., Noda, H., Noguchi, R., Ogawa, N., Ogawa, K., Okada, T., Okamoto, C., Ono, G., Ozaki, M., Saiki, T., Sakatani, N., Sawada, H., Senshu, H., Shimaki, Y., Shirai, K., Sugita, S., Takei, Y., Takeuchi, H., Tanaka, S., Tatsumi, E., Terui, F., Tsuda, Y., Tsukizaki, R., Wada, K., Watanabe, S., Yamada, M., Yamada, T., Yamamoto, Y., Yano, H., Yokota, Y., Yoshihara, K., Yoshikawa, M., Yoshikawa, K., Furuya, S., Hatakeda, K., Hayashi, T., Hitomi, Y., Kumagai, K., Miyazaki, A., Nakato, A., Nishimura, M., Soejima, H., Suzuki, A., Yada, T., Yamamoto, D., Yogata, K., Yoshitake, M., Tachibana, S., Yurimoto, H., 2022. Samples returned from the asteroid Ryugu are similar to Ivuna-type carbonaceous meteorites. Science 0, eabn7850. https://doi.org/10.1126/science.abn7850.